

# Search for axion resonances in vacuum birefringence with three-beam collisions

Stefan Evans<sup>1,\*</sup> and Ralf Schützhold<sup>1,2</sup>

<sup>1</sup>*Helmholtz-Zentrum Dresden-Rossendorf, Bautzner Landstraße 400, 01328 Dresden, Germany*

<sup>2</sup>*Institut für Theoretische Physik, Technische Universität Dresden, 01062 Dresden, Germany*

(Dated: October 18, 2023)

We consider birefringent (i.e., polarization changing) scattering of x-ray photons at the superposition of two optical laser beams of ultra-high intensity and study the resonant contributions of axions or axion-like particles, which could also be short-lived. Applying the specifications of the Helmholtz International Beamline for Extreme Fields (HIBEF), we find that this set-up can be more sensitive than previous light-by-light scattering (birefringence) or light-shining-through-wall experiments in a certain domain of parameter space. By changing the pump and probe laser orientations and frequencies, one can even scan different axion masses.

*Introduction* After the discovery of the Higgs particle [1], axions or axion-like particles are one of the most favorite candidates for new physics beyond the standard model. One way to motivate them is to consider the electromagnetic field strength tensor  $F_{\mu\nu}$  and its dual  $\tilde{F}_{\mu\nu}$  which can be contracted to yield the two lowest-order Lorentz invariants  $F_{\mu\nu}F^{\mu\nu} = 2(\mathbf{B}^2 - \mathbf{E}^2) = -\tilde{F}_{\mu\nu}\tilde{F}^{\mu\nu}$  as well as  $\tilde{F}_{\mu\nu}F^{\mu\nu} = -4\mathbf{B} \cdot \mathbf{E}$ . The former generates the Lagrangian density of electromagnetism while the latter is usually discarded because it is a total derivative. However, this argument is only valid if the pre-factor in front of this term  $\tilde{F}_{\mu\nu}F^{\mu\nu}$  is a constant. If this pre-factor is a dynamical field  $\phi$ , i.e., space-time dependent, this term does generate a non-trivial (effective) interaction Lagrangian of the form ( $\hbar = c = 1$ )

$$\mathcal{L}_{\text{int}} = g_\phi \phi \mathbf{B} \cdot \mathbf{E}, \quad (1)$$

where  $g_\phi$  denotes the (effective) interaction strength. Since the term  $\tilde{F}_{\mu\nu}F^{\mu\nu}$  is odd under parity  $\mathcal{P}$ , the axion field  $\phi$  is usually considered a pseudoscalar field.

Apart from this effective field theory approach, axions were originally proposed as a possible solution to the strong  $\mathcal{CP}$  problem in quantum chromodynamics (QCD), see, e.g., [2–8]. In the following, axions and axion-like particles will be used synonymously. Modeling the axion field as a massive scalar field weakly coupled to the other standard model particles, it could also be a candidate for dark matter [9–21] and would have important consequences for cosmology, see, e.g., [22–28].

In search of observable effects, astronomical data provide very important sources [29–31]. Similar to neutrinos, weakly coupled and long lived axions could provide a cooling mechanism for stars and other astrophysical objects (such as white dwarfs [32]), mostly due to their coupling (1) to photons. In fact, the apparent absence of such effects for our sun, for example, leads to significant restrictions on the parameter space of axions [33], see also [34, 35].

Nevertheless, such astronomical observations cannot supersede laboratory experiments. On the one hand, a direct and active experimental manipulation is qualita-

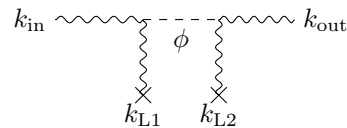


FIG. 1. Axion  $s$ -channel contribution to light-by-light scattering. The initial and final x-ray photons with momenta  $k_{\text{in}}$  and  $k_{\text{out}}$  interact with the fields of the two optical lasers  $k_{L1}$ ,  $k_{L2}$  via the internal axion propagator (dashed line).

tively different from an indirect observation, in particular since our conclusions drawn from the latter depend on our correct understanding of stellar dynamics etc. On the other hand, there are many reasons why axions detected in the laboratory could still be consistent with astronomical observations (especially if they occur on very different scales) [36–43], for example interaction effects such as running coupling constants or axion confinement [44–46].

The question of axion lifetimes and length scales distinguishes two major classes of laboratory-based experiments. Akin to astronomical searches, one class looks for long-lived axions propagating over macroscopic distances, including “light shining through wall” experiments [47–61] based on the creation of axions from electromagnetic fields via the coupling (1). Then, after propagating through the wall, the axion is converted back into an electromagnetic signal. A related but more indirect mechanism is based on detecting “missing photon energy”, e.g., at the BABAR experiment [62]. Photons produced in electron-positron collisions could undergo axion Bremsstrahlung [63]. The signature of the generated axions escaping the detector would then be an observable energy loss.

As a qualitatively different class of scenarios, sensitive to much smaller length scales, effective photon-photon interactions (light-by-light scattering) could be mediated by an internal axion line [64–77], see also Fig. 1. In this case, the axion does not propagate a macroscopic distance and thus such experiments would also be sensitive to axions which are not quasi-free and long-lived (at the scales relevant to the experiment).

Prominent examples for the second class are PVLAS [78–80], BMV [81–83] and OVAL [84]. Using a strong and static magnetic field as the pump field for polarizing the vacuum, the goal was to detect this change with an optical laser as the probe field. The sought-after signal was then a rotation or flip of the optical laser polarization, i.e., quantum vacuum birefringence.

In this work, we study an alternative scenario which is motivated by a recent proposal [85] for detecting quantum vacuum birefringence as predicted by quantum electrodynamics (QED). As the probe field, we envision x-ray photons generated by an x-ray free electron laser (XFEL) because their high frequency increases the signal. The pump field is supposed to be a superposition of two optical lasers, which offer pump field strengths much larger than in PVLAS. As already proposed in [85], the momentum exchange between the XFEL and the pump lasers facilitates a finite scattering angle (in the mrad regime) which helps us to discriminate the signal photons from the background (the main XFEL beam).

*Geometry* To illustrate our main idea, let us start with the most simple set-up. The initial x-ray photon is described by its energy  $\omega_{\text{in}}$ , momentum  $\mathbf{k}_{\text{in}} = \omega_{\text{in}} \mathbf{n}_{\text{in}}$ , polarization  $\mathbf{e}_{\text{in}}$ , and analogously for the final x-ray photon with  $\omega_{\text{out}}$ ,  $\mathbf{k}_{\text{out}} = \omega_{\text{out}} \mathbf{n}_{\text{out}}$  and  $\mathbf{e}_{\text{out}}$ , as well as for the two optical lasers with the same frequency  $\omega_{L1} = \omega_{L2} = \omega_L$ , but different propagation directions  $\mathbf{k}_{L1,2} = \omega_L \mathbf{n}_{L1,2}$  and polarizations  $\mathbf{e}_{L1,2}$ .

In order to obtain a resonant enhancement of our signal (see below), while also maximizing the deflection angle of the signal XFEL photon, we consider the case where an optical photon is absorbed from one laser and emitted into the other, such that energy and momentum conservation read

$$\begin{aligned} \omega_{\text{out}} &= \omega_{\text{in}} + \omega_{L1} - \omega_{L2} = \omega_{\text{in}} , \\ \mathbf{k}_{\text{out}} &= \mathbf{k}_{\text{in}} + \mathbf{k}_{L1} - \mathbf{k}_{L2} . \end{aligned} \quad (2)$$

Since we focus on the dominant (resonant) axion contribution and the birefringent  $\mathbf{e}_{\text{in}} \perp \mathbf{e}_{\text{out}}$  signal in or close to forward direction  $\mathbf{n}_{\text{in}} \approx \mathbf{n}_{\text{out}}$ , the direct interaction (1) between the initial and final x-ray photons is suppressed and hence we focus on the  $s$ -channel in Fig. 1 and neglect the  $t$ -channel.

As a consequence, each vertex (1) combines an x-ray photon with either of the two optical lasers. By adjusting the polarization and propagation unit vectors appropriately, we can select the various possibilities.

Let us first consider the fully perpendicular crossed-beam case  $\mathbf{n}_{L1,2} \perp \mathbf{n}_{\text{in}}$  where the two optical lasers collide head-on  $\mathbf{n}_{L1} = -\mathbf{n}_{L2}$ , see Fig. 3a. If we choose  $\mathbf{e}_{L1} = \mathbf{e}_{L2} = \mathbf{e}_{\text{in}}$ , there would be no axion contribution at all. Rotating the optical laser polarizations to  $\mathbf{e}_{L1} = \mathbf{e}_{L2} = \mathbf{n}_{\text{in}}$ , while keeping  $\mathbf{e}_{\text{in}}$  fixed, the axion interaction (1) would lead to scattering with the same polarization  $\mathbf{e}_{\text{out}} \parallel \mathbf{e}_{\text{in}}$ . A birefringent signal  $\mathbf{e}_{\text{out}} \perp \mathbf{e}_{\text{in}}$  could be obtained after rotating  $\mathbf{e}_{\text{in}}$  by  $45^\circ$  for example.

However, if we tilt the optical laser beams more towards the axis which is counter-propagating to the XFEL, as in Fig. 3c, the birefringent signal  $\mathbf{e}_{\text{out}} \perp \mathbf{e}_{\text{in}}$  would actually dominate for crossed optical laser polarizations  $\mathbf{e}_{L1} \perp \mathbf{e}_{L2}$  since then  $\mathbf{e}_{\text{out}}$  and  $\mathbf{e}_{\text{in}}$  could be aligned with either  $\mathbf{e}_{L1}$  or  $\mathbf{e}_{L2}$ , respectively.

*Axion Propagator* The lowest-order Feynman diagram of the process under consideration is displayed in Fig. 1. In terms of the momentum four-vectors  $\underline{k}_{\text{in}}$  and  $\underline{k}_{L1}$ , the four-momentum of the internal axion line reads  $\underline{p}_\phi = \underline{k}_{\text{in}} + \underline{k}_{L1}$  and thus its contribution to the amplitude becomes

$$\frac{g_\phi^2}{(\underline{k}_{\text{in}} + \underline{k}_{L1})^2 - m_\phi^2} = \frac{g_\phi^2}{2(\omega_{\text{in}}\omega_L - \mathbf{k}_{\text{in}} \cdot \mathbf{k}_{L1}) - m_\phi^2}, \quad (3)$$

where we have assumed that axion can be described by the standard propagator of a scalar field with mass  $m_\phi$ .

For the crossed-beam geometry discussed above, we have  $\mathbf{k}_{\text{in}} \perp \mathbf{k}_{L1}$  and thus the amplitude would be enhanced strongly near the resonance  $2\omega_{\text{in}}\omega_L \approx m_\phi^2$  corresponding to an axion mass of order  $\mathcal{O}(10^2 \text{ eV})$ . By varying the angles between the optical lasers and the XFEL, one can scan different axion masses (see below).

In fact, exactly on resonance  $2\omega_{\text{in}}\omega_L = m_\phi^2$ , the amplitude would actually diverge in the case of perfect plane waves. Of course, this implies that higher orders in  $g_\phi$  should be taken into account. A simple way of effectively doing this is to include self-energy terms in the propagator containing an imaginary part which then corresponds to a decay rate  $\Gamma_\phi \sim g_\phi^2$ . For plane waves, this would imply that the amplitude (3) is highly sensitive to the value of  $\Gamma$ . However, the optical laser is not a perfect plane wave, but a focused beam – with finite energy-momentum spread, which regularizes the amplitude (3). This removes dependence on  $\Gamma$  (unless it is larger than the energy-momentum spread of the optical laser) and thus accommodates both long and short-lived axions.

*Amplitude* Combining the coupling (1) with the propagator (3), the  $s$ -channel amplitude reads

$$\begin{aligned} \mathfrak{A}^s &= g_\phi^2 \frac{(\mathbf{e}_{\text{in}} \cdot [(\omega_{\text{in}}\mathbf{k}_{L1} - \omega_{L1}\mathbf{k}_{\text{in}}) \times \mathbf{A}_{L1}])}{2(\omega_{\text{in}}\omega_L - \mathbf{k}_{\text{in}} \cdot \mathbf{k}_{L1}) - m_\phi^2} \\ &\quad \times (\mathbf{e}_{\text{out}} \cdot [(\omega_{\text{out}}\mathbf{k}_{L2} - \omega_{L2}\mathbf{k}_{\text{out}}) \times \mathbf{A}_{L2}]), \end{aligned} \quad (4)$$

where  $\mathbf{A}_{L1,2}$  denote the vector potentials of the optical lasers. As explained above, the realistic description of a laser focus which is localized in space requires the average over a finite momentum spread  $\int d^3k_L$ , which we implement with a distribution function  $\mathbf{A}_L(\mathbf{k}_L)$ . This averaging procedure then also regularizes the resonant singularity of the axion propagator at  $2(\omega_{\text{in}}\omega_L - \mathbf{k}_{\text{in}} \cdot \mathbf{k}_{L1}) = m_\phi^2$ .

A finite temporal duration of the optical laser pulse would correspond to a spread in frequencies  $\omega_L = |\mathbf{k}_{L1,2}|$  but we neglect this spread here and focus on a fixed frequency  $\omega_L = |\mathbf{k}_{L1,2}|$  for simplicity.

*Experimental Parameters* Taking the specifications of the Helmholtz International Beamline for Extreme Fields (HIBEF) as an example, we consider the following experimental setup, as illustrated in Fig. 2. The optical lasers are characterized by their frequency  $\omega_L = 1.5$  eV, focus intensity  $\mathbf{E}^2 = 4 \times 10^{21} \text{W/cm}^2$ , with a  $3 \mu\text{m}$  waist and a divergence of  $\pm 15$  degrees. We model the optical laser focus by a superposition of plane waves with the same frequency  $\omega_L$  and a Gaussian distribution for the transversal momentum spread. Assuming a repetition rate of 5 Hz [86], one could carry out an experiment with  $\mathcal{O}(10^4)$  shots in less than one hour, such that we set  $\mathcal{O}(10^{-4})$  birefringent x-ray photons per shot as our detection threshold.

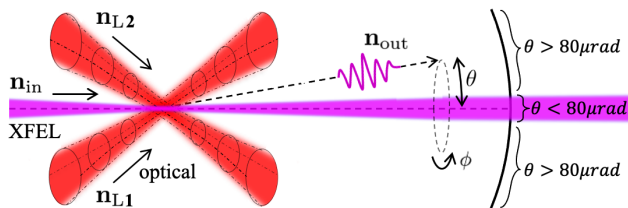


FIG. 2. Sketch of the experimental set-up.

We probe the optical laser background using an XFEL pulse of frequency  $\omega_{\text{in}} = 10$  keV, comprising  $N_{\text{XFEL}} = 10^{12}$  photons per shot, with a beam waist of  $5 \mu\text{m}$  and a  $80 \mu\text{rad}$  beam divergence [85, 86]. The combined momentum transfer supplied by pump field, being in the optical regime, scatters the XFEL photons outside of this  $80 \mu\text{rad}$  cone. Combining this consideration with energy-momentum conservation which allows a maximum scattering angle of  $300 \mu\text{rad}$ , we thus search for a signal between  $80 \mu\text{rad} < \theta < 300 \mu\text{rad}$ .

*Axion Signal* Now we are in the position to estimate the signal strength. As motivated above, we focus on the  $s$ -channel amplitude as the dominant contribution. Although only the case of the first photon being absorbed and the second one emitted yields a resonant enhancement and is thus the most important contribution, we also include the opposite (emission first) case for the sake of completeness and sum over both cases. Furthermore, we sum the diagram in Fig. 1 and the reverse sequence (exchanging the two optical lasers). Averaging the optical photons over the transversal momentum spread, we obtain the polarization-conserving ( $\mathbf{e}_{\text{in}} \parallel \mathbf{e}_{\text{out}}$ ) as well as birefringent ( $\mathbf{e}_{\text{in}} \perp \mathbf{e}_{\text{out}}$ ) differential cross sections as

$$\frac{d\sigma}{d\Omega} = \sum_{\pm} \frac{|\mathfrak{A}_{\pm}^s|^2}{4(2\pi)^3}, \quad (5)$$

where we have used that  $\omega_{\text{out}}/\omega_{\text{in}} \approx 1$ . Subscripts  $\pm$  label summation over both sequences of absorbed and emitted photons.

Given energy-momentum conservation, the XFEL can deflect to the left or right, e.g. parallel to the first (ab-

sorbed) optical photon and opposite the second (emitted), for the fully perpendicular case  $\mathbf{n}_{L1,2} \perp \mathbf{n}_{\text{in}}$  with  $\mathbf{n}_{L1} = -\mathbf{n}_{L2}$ . By tuning the polarizations, i.e. choosing which of  $\mathbf{e}_{L1}$  or  $\mathbf{e}_{L2}$  is aligned with  $\mathbf{e}_{\text{out}}$  or  $\mathbf{e}_{\text{in}}$ , we determine the sequence in which the photons interact and thus which way the signal photons deflect.

For pure plane waves, one could envision laser polarizations to be exactly aligned or orthogonal to the XFEL's, completely filtering the deflection in one direction. In our case however, the transversal momentum spread of the photons also means a distribution of their polarizations, so there is always some nonzero alignment with the XFEL polarization. Maximizing and minimizing the two laser alignments respectively allows us to tune the signal to prefer one direction by two orders of magnitude.

To determine the total number  $N_{\text{signal}}$  of signal photons, we integrate (5) over the domain of scattering angles discussed above  $80 \mu\text{rad} < \theta < 300 \mu\text{rad}$ . Taking into account the XFEL photon number  $N_{\text{XFEL}}$  per shot multiplied by the number  $10^4$  of shots and the size of the XFEL focus  $w_{\text{XFEL}} = 5 \mu\text{m}$ , we find

$$N_{\text{signal}} \approx 10^4 \frac{N_{\text{XFEL}}}{w_{\text{XFEL}}^2} \int_0^{2\pi} d\phi \int_{8 \cdot 10^{-5}}^{3 \cdot 10^{-4}} d\theta \sin \theta \frac{d\sigma}{d\Omega}. \quad (6)$$

As a function of  $m_\phi$ , the signal strength  $N_{\text{signal}}$  is peaked at resonance for a given laser geometry (3). Furthermore, the on-shell requirement for the XFEL and optical photons, e.g.,  $|\mathbf{k}_{L1}| = |\mathbf{k}_{L2}| = \omega_L$  in conjunction with energy-momentum conservation (2) generates a substructure consisting of much narrower peaks within the resonance. However, since the optical laser pulses will inevitably display small variations during the  $10^4$  shots, this small-scale substructure averages out – which we model by a Gaussian convolution.

In Fig. 3 we plot the domain of accessible axion parameter space as the coupling  $g_\phi$  and mass  $m_\phi$  for which  $N_{\text{signal}} \geq 1$  in (6), i.e., one or more signal photons per  $10^4$  XFEL shots. We display three optical laser orientations, the fully perpendicular case  $\mathbf{k}_{\text{in}} \perp \mathbf{k}_{L1,2}$ , here labeled  $\vartheta = \pi/2$ , as well as the cases  $\vartheta = 3\pi/4$  and  $\vartheta = 8\pi/9$ , where  $\vartheta$  denotes the angle between the optical laser and the XFEL.

As already discussed after Eq. (3), varying this angle effectively amounts to scanning different ranges of the axion mass. Indeed, when going from  $\vartheta = \pi/2$  to  $8\pi/9$ , the resonance shifts to higher axion masses and becomes more narrow. As a result, the enhancement of the signal at resonance increases. E.g., the case  $8\pi/9$  produces the strongest signal and is most sensitive to axion masses around  $m_\phi = 240$  eV.

Far away from resonance, i.e., at lighter or heavier axion masses, QED birefringence becomes important. For the parameters used here, it can be estimated from the Euler-Heisenberg-Schwinger effective action [87–89], see

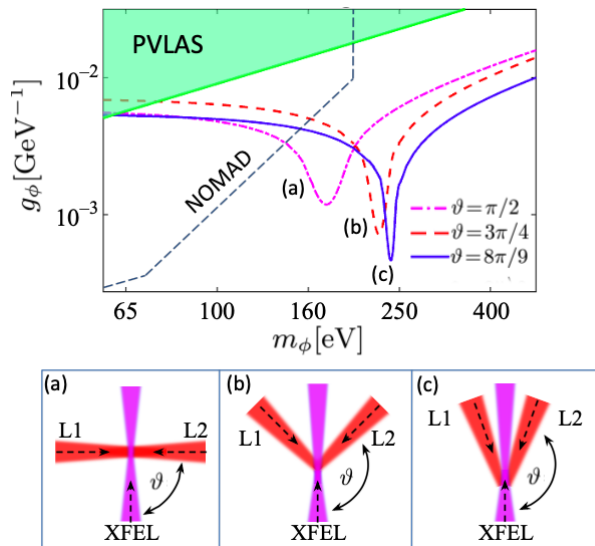


FIG. 3. Accessible parameter space based on  $N_{\text{signal}} \geq 1$  from Eq. (6) in terms of axion mass  $m_\phi$  and coupling  $g_\phi$ . The optical laser orientations relative to the XFEL (at  $\vartheta = 0$ ) are  $\vartheta = 8\pi/9$  (blue solid curve),  $\vartheta = 3\pi/4$  (red dashed curve) and  $\vartheta = \pi/2$  (purple dot-dashed curve). The green shaded region in the top left corner denotes the parameter region probed by PVLAS (birefringence [80]). The limits obtained by NOMAD (light-shining-through-wall [49]) are given by the black dashed curve.

also [85]. Near resonance, combining the axion and QED Feynman diagram can also generate interference effects, see Fig. 4.

So far we have considered exclusively the birefringent signal – one may also choose to include the polarization-conserving case as part of the desired signal. Applying e.g. polarizations  $\mathbf{e}_{L1} = \mathbf{e}_{L2} = \mathbf{n}_{\text{in}}$ , further enhancement of the signal strength is possible, since both lasers could then couple to the incoming XFEL, with their polarizations aligned to maximize the interaction. On the other hand, as discussed after Eq. (2), the choice  $\mathbf{e}_{L1} = \mathbf{e}_{L2} = \mathbf{e}_{\text{in}}$  suppresses the axion contribution, providing a diagnostic tool for filtering the pure QED signal.

*Conclusions* We have evaluated the axion contribution to birefringent light-by-light scattering for an XFEL probe and optical laser pump. Special emphasis is placed on the resonant axion contribution which allows us to scan different axion masses by changing the involved parameters such as the angle  $\vartheta$  between the XFEL and the optical laser. Furthermore, the axion resonance facilitates a sensitivity surpassing that of previous light-by-light scattering and light-shining-through-wall experiments such as PVLAS, BMV and NOMAD. Note that the parameters in Fig. 3, including the bounds from PVLAS and NOMAD, lie inside the region tested by BABAR and solar axion searches such as CAST. However, as explained above, these are more indirect tests which rely on various assumptions such as long lived axions. Thus,

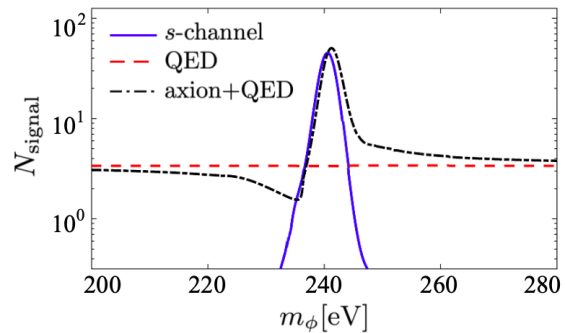


FIG. 4. Signal strength  $N_{\text{signal}}$  from (6) for  $\vartheta = 8\pi/9$ , plotted as a function of  $m_\phi$  at fixed coupling  $g_\phi = 10^{-3}\text{GeV}^{-1}$ . The solid blue curve represents the axion  $s$ -channel contribution alone while the black dot-dashed curve incorporates the combined effect of axion  $s$  and  $t$ -channels as well as the QED contribution (red dashed horizontal line).

the scheme presented here could provide the most stringent laboratory-based probe of short lived axion contributions.

Complementary to astrophysical bounds (e.g., [31]), such laboratory-based probes are also sensitive to axions which evade these bounds in some way. Examples could be interaction effects such as running coupling or confinement, see, e.g., [45, 46], which invalidate the picture of long-lived and free-streaming axions. Although we treated the axion field as a free massive scalar field for simplicity, our results can be generalized to this case by inserting the effective axion propagator into our amplitude. If this propagator displays one or more quasi-particle peaks, we would again obtain axion resonances. The width of these quasi-particle peaks (related to their life-time) would then be added to the width generated by the angular spread of the optical laser.

In view of the smallness of the signal, a discussion of its detectability should also include an estimate of possible background effects which might induce a false signal. These background effects are basically the same as already discussed in [85] devoted to the pure QED birefringence effect (see [87–109]). As discussed above, the axion signal displays distinctive dependence on the geometry (e.g., polarization directions), which could help to distinguish it from possible background effects.

In order to advance the sensitivity further, one could use more intense optical lasers (which will soon become available at HIBEF or at other facilities) or XFELs or tighten the XFEL beam waist [86], as well as increase the number of shots in the experiment.

*Acknowledgments* We thank N. Ahmadinia, T. Cowan, M. Ding, S. Franchino-Viñas, H. Gies, B. King, J. Grenzer, F. Karbstein, M. Lopez, R. Shaisultanov, M. Šmíd, and T. Toncia for fruitful discussions. This research was supported in part by Perimeter Institute for Theoretical Physics. Research at Perimeter

Institute is supported by the Government of Canada through the Department of Innovation, Science and Economic Development and by the Province of Ontario through the Ministry of Research and Innovation. R.S. acknowledges funding by the Deutsche Forschungsgemeinschaft (DFG, German Research Foundation) – Project-ID 278162697– SFB 1242.

---

\* s.evans@hzdr.de

- [1] P. W. Higgs, *Phys. Rev. Lett.* **13** (1964), 508-509
- [2] R. D. Peccei and H. R. Quinn, *Phys. Rev. Lett.* **38** (1977), 1440-1443
- [3] S. Weinberg, *Phys. Rev. Lett.* **40** (1978), 223-226
- [4] F. Wilczek, *Phys. Rev. Lett.* **40** (1978), 279-282
- [5] J. E. Kim, *Phys. Rev. Lett.* **43** (1979), 103
- [6] M. A. Shifman, A. I. Vainshtein and V. I. Zakharov, *Nucl. Phys. B* **166** (1980), 493-506
- [7] A. R. Zhitnitsky, *Sov. J. Nucl. Phys.* **31** (1980), 260
- [8] M. Dine, W. Fischler and M. Srednicki, *Phys. Lett. B* **104** (1981), 199-202
- [9] J. Preskill, M. B. Wise and F. Wilczek, *Phys. Lett. B* **120** (1983), 127-132
- [10] L. F. Abbott and P. Sikivie, *Phys. Lett. B* **120** (1983), 133-136
- [11] M. Dine and W. Fischler, *Phys. Lett. B* **120** (1983), 137-141
- [12] P. Sikivie, *Phys. Rev. Lett.* **51** (1983), 1415-1417
- [13] G. G. Raffelt, 1996, ISBN 978-0-226-70272-8
- [14] G. G. Raffelt, *Lect. Notes Phys.* **741** (2008), 51-71
- [15] A. Ringwald, *Phys. Dark Univ.* **1** (2012), 116-135
- [16] J. L. Ouellet *et al.* *Phys. Rev. Lett.* **122** (2019) no.12, 121802
- [17] A. Caputo, M. Regis, M. Taoso and S. J. Witte, *JCAP* **03** (2019), 027
- [18] G. Alonso-Álvarez, R. S. Gupta, J. Jaeckel and M. Spannowsky, *JCAP* **03** (2020), 052
- [19] P. Carenza, A. Mirizzi and G. Sigl, *Phys. Rev. D* **101** (2020) no.10, 103016
- [20] K. M. Backes *et al.* [HAYSTAC], *Nature* **590** (2021) no.7845, 238-242
- [21] Y. K. Semertzidis and S. Youn, *Sci. Adv.* **8** (2022) no.8, abm9928
- [22] J. Jaeckel and A. Ringwald, *Ann. Rev. Nucl. Part. Sci.* **60** (2010), 405-437
- [23] K. Baker *et al.* *Annalen Phys.* **525** (2013), A93-A99
- [24] I. G. Irastorza and J. Redondo, *Prog. Part. Nucl. Phys.* **102** (2018), 89-159
- [25] M. Buschmann, J. W. Foster and B. R. Safdi, *Phys. Rev. Lett.* **124** (2020) no.16, 161103
- [26] D. Cadamuro and J. Redondo, *JCAP* **02** (2012), 032
- [27] A. De Angelis, M. Roncadelli and O. Mansutti, *Phys. Rev. D* **76** (2007), 121301
- [28] J. F. Fortin, H. K. Guo, S. P. Harris, D. Kim, K. Sinha and C. Sun, *Int. J. Mod. Phys. D* **30** (2021) no.07, 2130002
- [29] R. Bernabei *et al.* *Phys. Lett. B* **515** (2001), 6-12
- [30] A. Ayala, I. Domínguez, M. Giannotti, A. Mirizzi and O. Straniero, *Phys. Rev. Lett.* **113** (2014) no.19, 191302
- [31] A. Ringwald, L.J Rosenberg and G. Rybka, “Axions and other similar particle,” Chapter 90 in: R. L. Workman *et al.* [Particle Data Group], *PTEP* **2022** (2022), 083C01
- [32] J. Isern, E. Garcia-Berro, S. Torres and S. Catalan, *Astrophys. J. Lett.* **682** (2008), L109
- [33] V. Anastassopoulos *et al.* [CAST], *Nature Phys.* **13** (2017), 584-590
- [34] E. Aprile *et al.* [XENON], *Phys. Rev. D* **102** (2020) no.7, 072004
- [35] J. B. Dent, B. Dutta, J. L. Newstead and A. Thompson, *Phys. Rev. Lett.* **125** (2020) no.13, 131805
- [36] M. Ahlers, H. Gies, J. Jaeckel and A. Ringwald, *Phys. Rev. D* **75** (2007), 035011
- [37] P. Brax, C. van de Bruck, A. C. Davis, D. F. Mota and D. J. Shaw, *Phys. Rev. D* **76** (2007), 124034
- [38] P. Brax, C. van de Bruck and A. C. Davis, *Phys. Rev. Lett.* **99** (2007), 121103
- [39] A. Dupays, E. Masso, J. Redondo and C. Rizzo, *Phys. Rev. Lett.* **98** (2007), 131802
- [40] H. Gies, J. Jaeckel and A. Ringwald, *Phys. Rev. Lett.* **97** (2006), 140402
- [41] J. Jaeckel, E. Masso, J. Redondo, A. Ringwald and F. Takahashi, *Phys. Rev. D* **75** (2007), 013004
- [42] Y. Liao, *Phys. Lett. B* **650** (2007), 257-261
- [43] R. N. Mohapatra and S. Nasri, *Phys. Rev. Lett.* **98** (2007), 050402
- [44] P. Jain and S. Mandal, *Int. J. Mod. Phys. D* **15** (2006), 2095-2104
- [45] E. Masso and J. Redondo, *JCAP* **09** (2005), 015
- [46] E. Masso and J. Redondo, *Phys. Rev. Lett.* **97** (2006), 151802
- [47] G. Ruoso *et al.* *Zeitschrift für Physik C Particles and Fields* **56** (1992), 505–508
- [48] R. Cameron *et al.* *Phys. Rev. D* **47** (1993), 3707-3725
- [49] P. Astier *et al.* [NOMAD], *Phys. Lett. B* **479** (2000), 371-380
- [50] M. Fouche *et al.* *Phys. Rev. D* **78** (2008), 032013
- [51] P. Pognat *et al.* [OSQAR], *Phys. Rev. D* **78** (2008), 092003
- [52] J. Redondo and A. Ringwald, *Contemp. Phys.* **52** (2011), 211-236
- [53] A. S. Chou *et al.* [GammeV (T-969)], *Phys. Rev. Lett.* **100** (2008), 080402
- [54] A. Afanasev, O. K. Baker, K. B. Beard, G. Biallas, J. Boyce, M. Minarni, R. Ramdon, M. Shinn and P. Slocum, *Phys. Rev. Lett.* **101** (2008), 120401
- [55] K. Ehret *et al.* *Phys. Lett. B* **689** (2010), 149-155
- [56] P. Pognat *et al.* [OSQAR], *Eur. Phys. J. C* **74** (2014) no.8, 3027
- [57] R. Ballou *et al.* [OSQAR], *Phys. Rev. D* **92** (2015) no.9, 092002
- [58] T. Inada *et al.* *Phys. Rev. Lett.* **118** (2017) no.7, 071803
- [59] T. Yamaji, K. Tamasaku, T. Namba, T. Yamazaki and Y. Seino, *Phys. Lett. B* **782** (2018), 523-527
- [60] K. A. Beyer, G. Marocco, R. Bingham and G. Gregori, *Phys. Rev. D* **105** (2022) no.3, 035031
- [61] M. D. Ortiz *et al.* *Phys. Dark Univ.* **35** (2022), 100968
- [62] M. J. Dolan, T. Ferber, C. Hearty, F. Kahlhoefer and K. Schmidt-Hoberg, *JHEP* **12** (2017), 094
- [63] Y. S. Tsai, *Phys. Rev. D* **34** (1986), 1326
- [64] L. Maiani, R. Petronzio and E. Zavattini, *Phys. Lett. B* **175** (1986) 359.
- [65] G. Raffelt and L. Stodolsky, *Phys. Rev. D* **37** (1988), 1237

- [66] Y. Semertzidis, R. Cameron, G. Cantatore, A. C. Melissinos, J. Rogers, H. Halama, A. Prodell, F. Nezirick, C. Rizzo and E. Zavattini, *Phys. Rev. Lett.* **64** (1990), 2988-2991
- [67] D. Bernard, *Nuovo Cim. A* **110** (1997), 1339-1346
- [68] S. Villalba-Chávez and A. Piazza, *JHEP* **11** (2013), 136
- [69] S. Villalba-Chávez, T. Podszus and C. Müller, *Phys. Lett. B* **769** (2017), 233-241
- [70] D. Tommasini, A. Ferrando, H. Michinel and M. Seco, *JHEP* **11** (2009), 043
- [71] B. Dobrich and H. Gies, *JHEP* **10** (2010), 022
- [72] S. Evans and J. Rafelski, *Phys. Lett. B* **791** (2019), 331-334
- [73] Z. Bogorad, A. Hook, Y. Kahn and Y. Soreq, *Phys. Rev. Lett.* **123** (2019) no.2, 021801
- [74] S. Shakeri, D. J. E. Marsh and S. S. Xue, [arXiv:2002.06123 [hep-ph]].
- [75] K. A. Beyer, G. Marocco, C. Danson, R. Bingham and G. Gregori, *Phys. Lett. B* **839** (2023), 137759
- [76] K. Homma *et al.* [SAPPHIRES], *JHEP* **12** (2021), 108
- [77] F. Ishibashi, T. Hasada, K. Homma, Y. Kirita, T. Kanai, S. Masuno, S. Tokita and M. Hashida, *Universe* **9** (2023) no.3, 123
- [78] E. Zavattini *et al.* [PVLAS], *Phys. Rev. Lett.* **96** (2006), 110406
- [79] E. Zavattini *et al.* [PVLAS], *Phys. Rev. D* **77** (2008), 032006
- [80] A. Ejlli, F. Della Valle, U. Gastaldi, G. Messineo, R. Pengo, G. Ruoso and G. Zavattini, *Phys. Rept.* **871** (2020), 1-74
- [81] R. Battesti, *et al.* *Eur. Phys. J. D* **46** (2008) 323-333
- [82] A. Cadène, P. Berceau, M. Fouché, R. Battesti and C. Rizzo, *Eur. Phys. J. D* **68** (2014), 16
- [83] R. Battesti *et al.* *Phys. Rept.* **765-766** (2018), 1-39
- [84] X. Fan *et al.* *Eur. Phys. J. D* **71** (2017) no.11, 308
- [85] N. Ahmadinia, T. E. Cowan, J. Grenzer, S. Franchino-Viñas, A. L. Garcia, M. Šmíd, T. Toncian, M. A. Trejo and R. Schützhold, *Phys. Rev. D* **108** (2023) no.7, 076005
- [86] U. Zastra *et al.* *J. Synchrotron Rad.* (2021). **28**, 1393-1416
- [87] W. Heisenberg and H. Euler, *Z. Phys.* **98**, 714 (1936).
- [88] V. Weisskopf, *Kong. Dan. Vid. Sel. Mat. Fys. Med.* **14**, N6, 1 (1936).
- [89] J. S. Schwinger, *Phys. Rev.* **82**, 664 (1951).
- [90] A. Di Piazza, K. Z. Hatsagortsyan and C. H. Keitel, *Phys. Rev. Lett.* **97** (2006), 083603
- [91] T. Heinzl, B. Liesfeld, K. U. Amthor, H. Schwöerer, R. Sauerbrey and A. Wipf, *Opt. Commun.* **267** (2006), 318-321
- [92] H. P. Schlenvoigt, T. Heinzl, U. Schramm, T. E. Cowan and R. Sauerbrey, *Phys. Scripta* **91** (2016) no.2, 023010
- [93] T. Inada, T. Yamazaki, T. Yamaji, Y. Seino, X. Fan, S. Kamioka, T. Namba and S. Asai, *Science* **7** (2017), 671
- [94] Y. Seino, T. Inada, T. Yamazaki, T. Namba and S. Asai, *PTEP* **2020** (2020) no.7, 073C02
- [95] F. Karbstein, D. Ullmann, E. A. Mosman and M. Zepf, *Phys. Rev. Lett.* **129** (2022) no.6, 061802
- [96] T. Inada *et al.* *Phys. Lett. B* **732** (2014), 356-359
- [97] E. Lundstrom, G. Brodin, J. Lundin, M. Marklund, R. Bingham, J. Collier, J. T. Mendonca and P. Norreys, *Phys. Rev. Lett.* **96** (2006), 083602
- [98] A. Di Piazza, A. I. Milstein and C. H. Keitel, *Phys. Rev. A* **76** (2007), 032103
- [99] B. King, H. Hu and B. Shen, *Phys. Rev. A* **98** (2018) no.2, 023817
- [100] D. Tommasini and H. Michinel, *Phys. Rev. A* **82** (2010), 011803
- [101] B. King and C. H. Keitel, *New J. Phys.* **14** (2012), 103002
- [102] H. Gies, F. Karbstein, C. Kohlfürst and N. Seegert, *Phys. Rev. D* **97** (2018) no.7, 076002
- [103] H. Gies, F. Karbstein and C. Kohlfürst, *Phys. Rev. D* **97** (2018) no.3, 036022
- [104] B. Dobrich and H. Gies, *EPL* **87** (2009) no.2, 21002
- [105] H. Gies, F. Karbstein and N. Seegert, *New J. Phys.* **17** (2015) no.4, 043060
- [106] H. Grote, *Phys. Rev. D* **91** (2015) no.2, 022002
- [107] S. Robertson *et al.*, *Phys. Rev. A* **103** (2021) no.2, 023524
- [108] H. Gies, F. Karbstein and L. Klar, *Phys. Rev. D* **106** (2022) no.11, 116005
- [109] F. Karbstein, C. Sundqvist, K. S. Schulze, I. Uschmann, H. Gies and G. G. Paulus, *New J. Phys.* **23** (2021) no.9, 095001